

# The elusive coordination of the $\text{Ag}^+$ ion in aqueous solution: evidence for a linear structure

Matteo Busato<sup>‡,†</sup>, Andrea Melchior<sup>‡</sup>, Valentina Migliorati<sup>†</sup>,  
Andrea Colella<sup>†</sup>, Ingmar Persson<sup>§</sup>, Giordano Mancini<sup>#</sup>,  
Daniele Veclani<sup>‡</sup>, Paola D'Angelo<sup>\*,†</sup>

<sup>‡</sup> Dipartimento Politecnico di Ingegneria e Architettura (DPIA),  
Laboratori di Chimica, Università di Udine,  
via delle Scienze 99, 33100 Udine, Italy

<sup>†</sup> Dipartimento di Chimica, Università di Roma "La Sapienza",  
P.le A. Moro 5, 00185 Roma, Italy

<sup>§</sup> Department of Chemistry and Biotechnology,  
Swedish University of Agricultural Sciences (SLU),  
SE-750 07 Uppsala, Sweden

<sup>#</sup> Centro HPC, Scuola Normale Superiore,  
Piazza San Silvestro 12, 56125 Pisa, Italy

\* [p.dangelo@uniroma1.it](mailto:p.dangelo@uniroma1.it)

E-mail:

---

\*To whom correspondence should be addressed

## Abstract

X-ray absorption spectroscopy (XAS) has been employed to study the coordination of the  $\text{Ag}^+$  ion in aqueous solution. The conjunction of extended X-ray absorption fine structure (EXAFS) and X-ray absorption near-edge structure (XANES) data analysis provided results suggesting the preference for a first shell linear coordination with a mean Ag-O bond distance of  $2.34(2) \text{ \AA}$ , different from the first generally accepted tetrahedral model with a longer mean Ag-O bond distance. *Ab initio* molecular dynamics simulations with the Car-Parrinello approach (CPMD) were also performed and were able to describe the coordination of the hydrated  $\text{Ag}^+$  ion in aqueous solution in very good agreement with the experimental data. The high sensitivity for the closest environment of the photoabsorber of the EXAFS and XANES techniques, together with the long-range information provided by CPMD and large angle X-ray scattering (LAXS), allowed us to reconstruct the three-dimensional model of the coordination geometry around the  $\text{Ag}^+$  ion in aqueous solution. The obtained results from experiments and theoretical simulations provided a complex picture with a certain amount of water molecules with high configurational disorder at distances comprised between the first and second hydration spheres. This evidence may have caused the proliferation of the coordination numbers that have been proposed so far for  $\text{Ag}^+$  in water. Altogether these data show how the description the hydration of the  $\text{Ag}^+$  ion in aqueous solution can be complex, differently from other metal species where hydration structures can be described by clusters with well-defined geometries. This diffuse hydration shell causes the Ag-O bond distance in the linear  $[\text{Ag}(\text{H}_2\text{O})_2]^+$  ion to be ca.  $0.2 \text{ \AA}$  longer than in isolated ions in solid state.

## Introduction

Water is the most abundant compound on the surface of the Earth, being the principal constituent of living organisms and the basis of life on our planet. As a matter of fact, knowledge of the structural properties of water is central in many issues related to physics, chemistry and biology. Even if water has an apparently simple molecular structure, it is a rather complex medium and the description of its structural features is often a difficult task. This can be particularly true when its

internal structure is influenced by external agents like temperature and pressure changes, as well as by internal ones such as the presence of solutes. Among these latter, water can be dramatically affected by the presence of ions.<sup>1</sup>

All ions are hydrated to varying extent in water, but the hydration strength can depend on many factors, such as charge density and polarizability. Furthermore, ions in water can behave both as structure makers or breakers, making the description of their aqueous surroundings a non-trivial task.<sup>2</sup> The structural and dynamic properties of the hydration spheres of aqua-ions are fundamental to understand the behavior of chemical and biological systems and processes. In addition, a complete understanding of metal ion coordination in aqueous solution can be an essential starting point for the comprehension of its properties even in other molecular solvents. In this framework, even though the coordination properties of the  $\text{Ag}^+$  ion in water have been widely investigated for many years, its hydration structure in solution is still elusive. In particular, its hydration number, as well as the average bond distance with the first hydration shell water molecules, are far from being unambiguously determined.<sup>3-8</sup>

In the last decades, both experimental and theoretical studies have been devoted to the hydration properties of the  $\text{Ag}^+$  ion. As regards the earliest works, the general picture arising from experimental techniques is that of a tetrahedrally-coordinated metal ion. This is the case of neutron diffraction studies on concentrated solutions of silver nitrate<sup>3</sup> and perchlorate<sup>4</sup> reporting coordination numbers (CN) of 3.7(5) and 4.1(3), and a mean distance between the  $\text{Ag}^+$  ion and the oxygen atoms of the water molecules (Ag-O) within the first hydration shell of 2.40(2) and 2.41(2) Å, respectively.

Extended X-ray absorption fine structure (EXAFS) spectroscopy has also been employed to determine the hydration properties of the  $\text{Ag}^+$  ion. Yamaguchi and co-workers<sup>5</sup> found the  $\text{Ag}^+$  ion to be coordinated by three to four water molecules at Ag-O distances of 2.31 Å and 2.36 Å for 3 M and 9 M solutions of silver nitrate and perchlorate, respectively. In addition, Funahashi *et al.*<sup>6</sup> carried out an EXAFS study of the  $\text{Ag}^+$  ion in water and reported a CN of 4.0 with a Ag-O distance of 2.41 Å, even though the authors pointed out that these structural parameters were

kept fixed during the fitting procedure.

This assumption of a tetrahedral coordination for the solvated  $\text{Ag}^+$  ion was often employed for the interpretation of complex formation thermodynamics.<sup>9</sup> In particular, the thermodynamic parameters for the formation of  $\text{Ag}^+$  complexes with simple N-donor ligands (*e.g.* L = ammonia, pyridine) were compatible with a change of coordination mode of the metal ion from a starting tetrahedral to a linear geometry in the  $\text{AgL}_n^+$  species.<sup>9-11</sup>

On the other hand, more recent studies started questioning the tetrahedral model. Persson and co-workers<sup>7</sup> found that a "2 + 2" structure with two water molecules coordinating  $\text{Ag}^+$  at 2.32 Å and two at 2.48 Å, was able to provide a better fit of the EXAFS and large-angle X-ray scattering (LAXS) experimental data with respect to a regular tetrahedral model. The authors described this cluster as a tetrahedral structure distorted towards a linear one. However, they pointed out that the number of water molecules set at long distance remains uncertain, and that a mean number larger than two could be expected. In fact, the LAXS and EXAFS techniques are known to be complementary, being LAXS more sensitive to long and weak interactions, and EXAFS to short and well-defined distances.<sup>7</sup> The authors underlined that it was not possible to provide a definite geometry of this "2 + 2" cluster in terms of bond angles, since no multiple-scattering (MS) effects were found detectable in the inner coordination sphere observed by EXAFS due to lack of symmetry while, for the same reason, no oxygen-oxygen distances were observed by LAXS.

Differently, Fulton and co-workers<sup>8</sup> suggested the occurrence in solution of clusters with CNs of 5 and 6, *i.e.* of either a trigonal bipyramidal or octahedral coordination on the basis of Ag K- and L<sub>2</sub>-edge EXAFS data.

High CN values have been often obtained also by many theoretical works. Both classical methods, such as molecular dynamics (MD) or Monte Carlo simulations or even techniques at quantum-mechanical level reproduced a  $\text{Ag}^+$  ion coordinated by at least five or six water molecules with Ag-O distances ranging from 2.3 to 2.6 Å.<sup>12-17</sup> In addition, the parametrization of  $\text{Ag}^+$ -water interaction potentials with the aim of reproducing the hydration properties of this ion has been an

effort of many groups.<sup>12,14,18</sup> However, the simultaneous reproduction of some target parameters altogether, such as the metal ion coordination number, average bond distance with water and hydration free energy ( $\Delta G_{hyd}$ ), was found to be out of the reach of classical interaction potentials. Spezia *et al.*<sup>14</sup> obtained Lennard-Jones (LJ) parameters able to reproduce a bond distance of 2.36 Å and the  $\Delta G_{hyd}$ , but a CN of 5.5 was also obtained, while the goal of the fitting procedure was CN = 4.0. In a more recent work, Merz and Li<sup>18</sup> proposed two sets of LJ parameters for the  $\text{Ag}^+$  ion: the first providing a good  $\Delta G_{hyd}$ , but underestimating the Ag-O distance (2.10 - 2.14 Å) with a CN of 4.9 - 5.3 and a second providing a good bond distance (2.40 Å), but underestimated  $\Delta G_{hyd}$  and a CN close to 6. The employment of more complex, but still classical functional forms, such as  $r^{-n}$  polynomials (with  $n = 6, 8, 9, 12$ ) for the van der Waals (vdW) interactions, were not able to address this issue.<sup>12</sup> In fact, also in this latter study a high CN of 4.9 was obtained, alongside with a Ag-O bond of 2.59 Å.

Altogether these results show how the reproduction of the peculiar hydration properties of this metal ion should need an explicit description of the electronic degrees of freedom. In this respect, Vuilleumier and Sprik<sup>15</sup> employed Car-Parrinello molecular dynamics (CPMD) to simulate one  $\text{Ag}^+$  ion immersed in a box of 33 water molecules that provided a CN of 5. When one water molecule was removed from the system, a CN = 4 was obtained, highlighting how the definition of the simulation parameters is crucial in such methods.

The  $\text{Ag}^+$  ion has a  $[Kr]4d^{10}5s^1$  ground state configuration, which is believed to undergo hybridization between the  $4d_z^2$  and  $5s$  orbitals promoted by a contraction of the  $5s$  orbital because of relativistic effects. The resulting  $sd_z^2$  hybrid orbital presents a shifted electron density from the  $d_z^2$  lobes to the toroid that generates two areas of reduced electron density along the  $z$ -axis.<sup>10</sup> This should lead to a strong tendency to form 2-fold coordination structures in a linear geometry. However, while this effect is well-known for  $\text{Au}^+$ , which forms several linear complexes because of marked relativistic effects,<sup>19</sup> the situation is more uncertain for  $\text{Ag}^+$ , being this a second-row transition metal.

Experimentally, linear  $[\text{Ag}(\text{H}_2\text{O})_2]^+$  configurations are observed at the solid state<sup>20-29</sup> and

here the structure of the hydrated  $\text{Ag}^+$  ion displays an unusual patterns for what concerns the Ag-O distance. In particular, the mean Ag-O bond in  $[\text{Ag}(\text{H}_2\text{O})_2]^+$  complexes without any other atoms within the vdW radii is 2.128 Å (Table S1).<sup>20,22–25</sup> However, when  $\text{Ag}^+$  presents only very weak interactions, the Ag-O distance increases of even more than 0.1 Å in the still linear  $[\text{Ag}(\text{H}_2\text{O})_2]^+$  ion (Table S1).<sup>21,26</sup> Differently, the Ag-O bond distance as determined by EXAFS and LAXS for hydrated silver(I) in aqueous solution where  $\text{Ag}^+$  has been proposed as linear or *quasi*-linear is slightly longer than 2.3 Å.<sup>5,7</sup> This shows that the Ag-O bond can be very different depending upon the occurrence of very weak interactions with neighboring atoms within the vdW distance, this kind of behavior being peculiar of the silver(I) ion. On the other hand, hydrated four-fold  $\text{Ag}^+$  ions have been reported in three different solid compounds. In one case, one  $[\text{Ag}(\text{H}_2\text{O})_4]^+$  complex has been presented as an independent unit with a mean Ag-O bond of 2.395 Å, but with a very broad distance distribution (2.248 - 2.629 Å) as well as for the O-Ag-O angle (89.1° - 129.0°).<sup>27</sup> In the other two structures, polymeric chains have been observed where two water molecules bridge two  $\text{Ag}^+$  ions in almost square-planar  $[\text{Ag}_2(\text{H}_2\text{O})_2]^{2+}$  units with mean Ag-O bond distances of 2.432 and 2.469 Å.<sup>28,29</sup>

The stability of the  $[\text{Ag}(\text{H}_2\text{O})_2]^+$  species has been also argued by the study of experimental incremental enthalpies for  $[\text{Ag}(\text{H}_2\text{O})_n]^+$  ( $n = 2 - 6$ ) clusters, showing that the first two water molecules are bound to silver more tightly than the remaining four.<sup>30</sup> A similar result has been obtained by Iino *et al.*<sup>31</sup> by means of IR spectroscopy on laser-vaporized clusters, showing that di-coordinated  $\text{Ag}^+$  isomers were identified in addition to tri-coordinated structures, and that the introduction of the fourth water molecule induced the revival of the two-fold coordination. From a theoretical point of view, density functional theory (DFT) calculations on the same incremental clusters have reported different results depending on the employed theoretical model. While some authors have found that the most stable coordination is represented by the three-fold  $[\text{Ag}(\text{H}_2\text{O})_3]^+$  species,<sup>32</sup> others have argued that the binding energy for the addition of the third water is close to zero or even positive, or that the energetic cost of placing the third water molecule directly bound to silver or in the second solvation shell is essentially the same.<sup>10,33</sup>

In this work, a study combining X-ray absorption spectroscopy (XAS) with *ab initio* MD simulations is carried out to shed light on the elusive hydration structure of the  $\text{Ag}^+$  ion. A re-evaluation of the LAXS data originally reported in Ref.<sup>7</sup> has been made on the light of the results obtained by the MD simulations in this study. The difficulty in obtaining accurate results on metal ion solvation structures in disordered liquid systems is well-known,<sup>34</sup> therefore we used both the EXAFS and the XANES (X-ray absorption near-edge structure) techniques to obtain a unified picture of the hydration structure. XAS spectroscopy is known to be a very powerful tool for the study of the first shell structure surrounding a metal, owing to its high sensitivity to the closest environment of the photoabsorber.<sup>35,36</sup> The LAXS technique provides vital information about long and diffuse distances not possible by XAS. In particular, the low energy part of a XAS spectrum provides unique information about the three-dimensional arrangement of the scattering atoms,<sup>34</sup> and to the best of our knowledge, this is the first time that XANES is employed in the study of  $\text{Ag}^+$  coordination in water. At the same time, *ab initio* simulations with the Car-Parrinello approach were performed on a system formed by one  $\text{Ag}^+$  and 99 water molecules to obtain further insights into the  $\text{Ag}^+$  hydration properties and to assess the reliability of the XAS experimental results. This combined approach exploiting both the sensitivity of the XANES spectroscopy towards the local arrangement around the photoabsorber in liquids and the ability of *ab initio* simulation to properly treat the valence electrons quantum-mechanically, allows us to find a robust hydration model for the  $\text{Ag}^+$  ion in water.

## Methods

### X-Ray Absorption Measurements

A weighed amount of anhydrous silver perchlorate  $\text{AgClO}_4$  (G. F. Smith) was dissolved in Millipore Q filtered water to obtain a  $0.2 \text{ mol} \cdot \text{dm}^{-3}$  solution. Ag K-edge XAS spectra were collected in transmission mode at the wiggler beam line 4-1 of the Stanford Synchrotron Radiation Laboratory (SSRL). The EXAFS beam line was equipped with a Si(220) double-crystal monochromator

while the storage ring was operating at 3.0 GeV with a maximum current of 100 mA. Higher order harmonics were reduced by detuning the second crystal to achieve 70% of the maximum intensity at the end of the scans. The energy scale of the XAS spectra was calibrated by assigning the first inflection point of the K-edge of a silver foil to 25514 eV.<sup>37</sup> Three spectra were collected and averaged to obtain a satisfactory signal-to-noise ratio.

## EXAFS Data Analysis

The analysis of the EXAFS data was carried out by means of the GNXAS program that is based on the calculation of a theoretical signal and a subsequent refinement of the structural parameters to obtain the best agreement with the experimental data.<sup>38,39</sup> In this approach, the interpretation of the experimental data is based on the decomposition of the  $\chi(k)$  signal into a summation over n-body distribution functions calculated by means of the MS theory.

The amplitude function  $A(k, r)$  and phase shifts  $\phi(k, r)$  have been calculated from clusters with fixed geometry with muffin-tin (MT) potentials and advanced models for the exchange-correlation self-energy (Hedin-Lundqvist), which allowed us to take into account photoelectron inelastic losses intrinsically.<sup>40</sup> To this extent, two structures consisting of a linear  $[\text{Ag}(\text{H}_2\text{O})_2]^+$  and a trigonal bipyramidal  $[\text{Ag}(\text{H}_2\text{O})_5]^+$  cluster were employed to take into account the low and high CN cases, as it is known that the potential is only weakly dependent on the selected geometry.<sup>41</sup> MT radii were chosen to obtain a 20% overlap of the MT spheres. To this purpose MT radii of 1.91, 0.90 and 0.20 Å were used for silver, oxygen and hydrogen atoms, respectively.

The theoretical signal  $\chi(k)$  is related to the experimental absorption coefficient  $\alpha(k)$  through the relation  $\alpha(k) = J\sigma_0(k)[1+S_0^2\chi(k)]+\beta(k)$ , where  $\sigma_0(k)$  is the atomic cross section,  $J$  is the edge jump,  $S_0^2$  provides a uniform reduction of the signal and is associated with many-body corrections to the one-electron cross section, and  $\beta(k)$  is the background function accounting for further absorbing processes. Multielectron excitation channels are accounted for by modeling the  $\beta(k)$  function as the sum of a smooth polynomial spline plus step-shaped functions.

In the present study the Ag-O first coordination shell has been modeled with  $\Gamma$ -like functions



which depend on four parameters, namely the coordination number CN, the average distance R, the Debye-Waller factor  $\sigma^2$  and the skewness  $\beta$ . The  $\beta$  parameter is related to the third cumulant  $C_3$  of the distance distribution through the relation  $C_3 = \sigma^3 \beta$ , and R is its first moment. Both the Ag-O and the Ag-H two body signals have been included in the calculation. The three-body distributions associated with O-Ag-O configurations have also been considered, but the amplitude of the theoretical signals has been found to be negligible. Least-squares fits have been carried out directly on the raw data, without preliminary background subtraction or Fourier filtering, by minimizing a residual function  $R_{sq}$  running over the squares of the differences between the experimental  $\alpha_m(E_i)$  spectral points and the model  $\alpha_m(E_i, \lambda)$  which depends on the ensemble of the optimized parameters  $\lambda$ , according to the equation:

$$R_{sq} = \sum_i [\alpha(E_i) - \alpha_m(E_i, \lambda)]^2 \times W(E_i) \quad (1)$$

where  $W(E_i)$  is a statistical weight. During the fit, all the structural parameters have been optimized with the exception of CN, which has been constrained with values ranging from 1.0 to 6.0 every 0.1 units in order to determine the best-fitting CN for the  $\text{Ag}^+$  ion in water. In addition, non-structural parameters have been optimized, namely  $E_0$  which is the K-edge ionization energy, and the  $\text{KN}_1$  and  $\text{KM}_{4\&5}$  double-electron excitation channel parameters placed respectively at 110 and 409 eV above the threshold energy on the basis of the  $Z + 1$  approximation. The inclusion of the double-excitations allowed us to keep the amplitude reduction factor  $S_0^2$  always constrained to 0.99.

## XANES Data Analysis

The XANES data analysis has been carried out using the MXAN code.<sup>42</sup> The potential has been calculated in the framework of the MT approximation using a complex optical potential, based on the local density approximation of the excited photoelectron self-energy. The MT radii were 1.89 Å for silver, 0.90 Å for oxygen and 0.20 Å for hydrogen. The real part of the self-energy was

calculated by the  $X_\alpha$  approximation, while inelastic losses were accounted for by convolution of the theoretical spectrum with a Lorentzian function having an energy-dependent width of the form  $\Gamma_{tot}(E)=\Gamma_c+\Gamma_{mfp}(E)$ . The constant part  $\Gamma_c$  includes the core-hole lifetime (6.75 eV FWHM), while the energy-dependent term  $\Gamma_{mfp}(E)$  represents all the intrinsic and extrinsic inelastic processes. The function  $\Gamma_{mfp}(E)$  is zero below an onset energy  $E_s$  and begins to increase from a value  $A_s$ , following the universal functional form of the mean free path in solids. The numerical values of  $E_s$  and  $A_s$  were derived at each computational step using a Monte Carlo fit. A Gaussian convolution was used to account for the experimental resolution.

Different starting models of the  $Ag^+$  hydration complex have been used to calculate the corresponding theoretical spectra and the hydrogen atoms have been considered in the analysis. Only the first hydration shell has been included in the analysis.

Least-squares fits have been carried out in order to optimize the geometry of the starting models and the nonstructural parameters using a residual function defined as:

$$R_{sq} = \frac{\sum_{i=1}^m w_i (y_i^{th} - y_i^{exp})^2}{\varepsilon_i^2 \sum_{i=1}^m w_i} \quad (2)$$

where  $m$  is the number of data points,  $y_i^{th}$  and  $y_i^{exp}$  are the theoretical and experimental values of absorption, respectively,  $\varepsilon_i$  is the individual error in the experimental data set, and  $w_i$  is a statistical weight. Five nonstructural parameters have been optimized, namely the experimental resolution  $\Gamma_{exp}$ , the Fermi energy level  $E_F$ , the threshold energy  $E_0$ , the energy and amplitude of the plasmon  $E_s$  and  $A_s$ .

## Large Angle X-ray Scattering

The LAXS data on an aqueous  $2.0 \text{ mol}\cdot\text{dm}^{-3}$  silver(I) perchlorate solution, acidified with  $0.1 \text{ mol}\cdot\text{dm}^{-3}$ , originally presented in Ref.<sup>7</sup> have been re-evaluated. All details about the experiment are available in Ref.<sup>7</sup> The model of the hydrated  $Ag^+$  ion used in the LAXS data analysis will be

explained in details in the Results and Discussion section.

## Car-Parrinello Molecular Dynamics Simulations

*Ab initio* MD simulations of the  $\text{Ag}^+$  ion in aqueous solution have been carried out with the Car-Parrinello approach by means of the CPMD 4.1 code.<sup>43</sup> The BLYP functional combining Becke's Generalized Gradient Approximation (GGA)<sup>44</sup> for exchange and Lee-Yang-Parr<sup>45</sup> for correlation energies has been employed with Grimme's empirical corrections for dispersion.<sup>46</sup>

Norm-conserving pseudopotentials of the Martins-Troullier type<sup>47</sup> were used for all the atoms. Kohn-Sham orbitals for valence electrons were expanded in a plane-waves basis set truncated at a cutoff energy of 70 Ry. The Kleinman-Bylander transformation<sup>48</sup> was employed for the non-local part of the pseudopotentials. A fictitious mass of 400 a.u. was associated to the electronic degrees of freedom and a time step of 4 a.u. (0.097 fs) was employed for all the simulations. These fictitious mass and time step, along with the whole level of theory, have been previously demonstrated to provide good results for bulk water structural description<sup>49-52</sup> and have been already employed in the study of ions coordination in aqueous solution.<sup>53-55</sup> Note that both the fictitious mass and time step are smaller than those employed by Vuilleumier and Sprik<sup>15</sup> in their CPMD simulation of  $\text{Ag}^+$  in water.

One  $\text{Ag}^+$  ion was put in the middle of a periodic cubic box of 14.7 Å edge and surrounded by 99 water molecules. The box size and number of molecules were set to reproduce water density at 300 K. In addition, a  $\text{Cl}^-$  ion was added in order to counterbalance the total positive charge of the system. The positions of the  $\text{Ag}^+$  and  $\text{Cl}^-$  ions were fixed at the center and one corner of the box, respectively, thus minimizing as much as possible their reciprocal interaction and avoiding chloride coordination towards silver. The distance between the two ions resulted of 11 Å and was preserved during all simulation time. This strategy of introducing a counter ion was observed to be mandatory to obtain an accurate reproduction of  $\text{Ag}^+$  coordination in comparison with the experimental data (*vide infra*). To check the goodness of this simulation protocol, a second system consisting of one  $\text{Ag}^+$  ion and 100 water molecules (*i.e.* without counter ion) was also simulated.

In both simulations the system was initially prepared by running a 10 ns classical MD run in NVT conditions at 300 K with the GROMACS 5.1.6 software.<sup>56</sup> The SPC/E water model<sup>57</sup> was employed along with LJ parameters for  $\text{Ag}^+$  that were observed to reproduce a CN of 4.0 and an Ag-O distance of 1.91 Å ( $\sigma = 1.50$  Å,  $\epsilon = 0.4$  kJ mol<sup>-1</sup>). This protocol was chosen in order to obtain an equilibrated starting configuration carrying a tetrahedrally-coordinated  $\text{Ag}^+$ . Successively, a wave-function optimization was carried out with the CPMD code, followed by a 2 ps equilibration in the microcanonical ensemble. A production run for data collection was then performed in NVT conditions at 300 K for 35 ps. Temperature of the nuclei was kept constant by coupling the ionic subsystem to the Nosé-Hoover thermostat with a frequency of 1500 cm<sup>-1</sup>. No thermostat was associated to the electronic degrees of freedom. The electronic kinetic energy has been constantly monitored and it did not show any relevant drift during all simulation time. The VMD 1.9.3 software<sup>58</sup> was employed for trajectories visualization and the TRAVIS code<sup>59</sup> for the analysis. For the calculation of the instantaneous coordination numbers, an in-house code has been used.

## Results and discussion

### Determination of $\text{Ag}^+$ hydration structure by EXAFS

To first assess the ability of the EXAFS technique to determine the  $\text{Ag}^+$  hydration structure, several minimization procedures have been carried out on the Ag K-edge X-ray absorption spectrum of a 0.2 mol·dm<sup>-3</sup>  $\text{AgClO}_4$  aqueous solution by keeping fixed the CN to determinate values and optimizing all the other parameters. To this purpose, two-body theoretical signals associated with the Ag-O and Ag-H first shell contributions have been calculated, while the amplitude of the signals arising from the second shell oxygen atoms has turned out to be negligible. Least-squares fits were performed in the 2.7 - 15.0 Å<sup>-1</sup>  $k$ -range for fixed CNs of the  $\text{Ag}^+$  ion comprised between 1.0 and 6.0, while the Ag-O and Ag-H distances and Debye-Waller factor values were optimized together with the non-structural parameters. The fit of the experimental data provided an  $E_0$  value of 3.8

eV above the first inflection point of the experimental spectrum, while the energy positions of the  $\text{KN}_1$  and  $\text{KM}_{4\&5}$  double-electron excitation channels were found at 94 and 418 eV, respectively

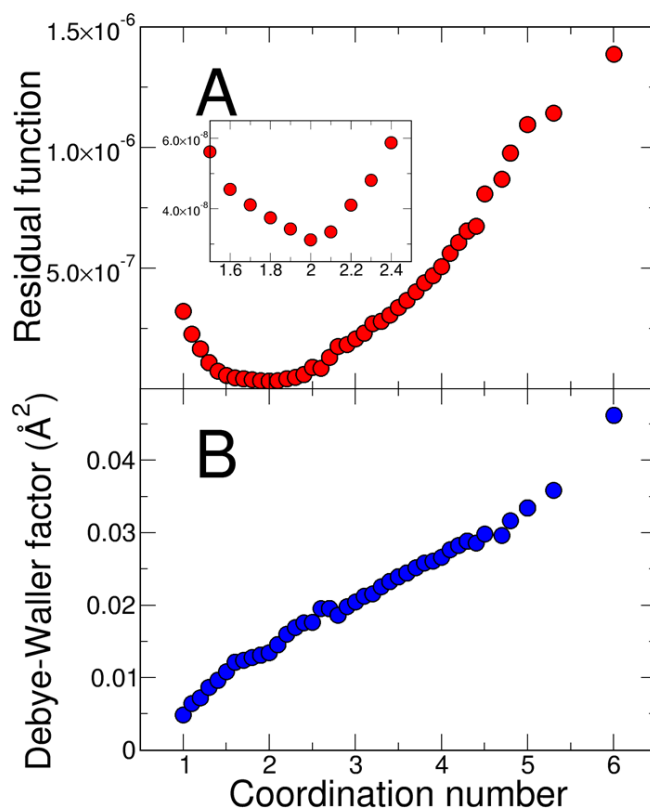


Figure 1: Residual function  $R_{sq}$  (A) and Debye-Waller factor  $\sigma^2$  (B) obtained from the analysis of the Ag K-edge EXAFS spectrum of a  $0.2 \text{ mol} \cdot \text{dm}^{-3}$   $\text{AgClO}_4$  aqueous solution as a function of  $\text{Ag}^+$  coordination number. In the A panel, an inset focusing on the obtained minimum values of  $R_{sq}$  is also reported.

Figure 1A shows the value of the residual function  $R_{sq}$  obtained from the minimization procedures as a function of the first shell Ag-O coordination number. As can be observed, the smallest residual between the theoretical and experimental spectra is obtained for a Ag-O CN of 2.0, while  $R_{sq}$  tends to increase exponentially for higher CN values. This first finding suggests a picture of a two-fold hydration complex formed by the  $\text{Ag}^+$  ion in aqueous solution, at variance with the previous EXAFS determinations.<sup>5,6,8</sup> In addition, the Debye-Waller factor values associated with the Ag-O two body signal obtained from the minimization procedures have been plotted as a function of CN in Figure 1B. It is well known that in the EXAFS analysis there is a high correlation between

the Debye-Waller factor and the coordination number, as both parameters affect the amplitude of the  $\chi(k)$  signal.<sup>34</sup> As a consequence, while the EXAFS technique shows a picometric sensitivity on the determination of the first shell distance, the number of atoms coordinating the photoabsorber can difficultly be extracted with high accuracy. As expected, Figure 1B shows a linear correlation between these two parameters, with  $\sigma^2$  values that tend to increase with increasing CNs. The Debye-Waller coefficient,  $\sigma^2$ , of the Ag-O bond distance at CN=2 (0.013(2) Å<sup>2</sup>) is larger than normally observed for e.g. hexahydrated transition metal ions (ca. 0.008 Å<sup>2</sup>).<sup>34,60–63</sup> This strongly indicates that the Ag-O bond is weak, especially when the low CN is taken into account. When increasing the CN as fixed value in the refinements,  $\sigma^2$  tends to increase to unreasonable values close to 0.05 Å<sup>2</sup> for CNs near 6.0 (Figure 1B).

As a result, it can be concluded that the best fit for the EXAFS part of the spectrum is provided by a CN value of 2.0. The upper panel of Figure 2 shows the comparison between the experimental spectrum and the theoretical  $\chi(k)$  curve obtained for the Ag-O CN value of 2.0. The first two curves from the top are the Ag-O and Ag-H two body first shell contributions, while the reminder of the figure shows the total theoretical signal compared with the experimental data and the resulting residuals. A complete list of the optimized parameters is reported in Table 1. As can be observed, a very good agreement is obtained between the EXAFS theoretical and experimental spectra, the validity of the analysis being furtherly reinforced by the comparison between the Fourier transform (FT) moduli shown in the lower panel of Figure 2. FT spectra have been calculated in the  $k$ -range 2.7-15.0 Å<sup>-1</sup> with no phase-shift correction applied. The results of the EXAFS analysis carried out by fixing the CN value to 4 are shown in Figure S1 of the Supporting Information. In this case a worse agreement between the theoretical and experimental curves can be observed.

**Table 1: Structural parameters obtained from the EXAFS analysis on the Ag K-edge EXAFS spectrum of a 0.2 mol·dm<sup>-3</sup> AgClO<sub>4</sub> aqueous solution. CN is the coordination number, R is the average distance,  $\sigma^2$  is the Debye-Waller factor and  $\beta$  is the asymmetry index.**

	CN	R (Å)	$\sigma^2$ (Å <sup>2</sup> )	$\beta$
Ag-O	2.0(3)	2.34(2)	0.013(2)	0.1(1)
Ag-H	4.0(6)	3.02(2)	0.020(3)	0.0(1)

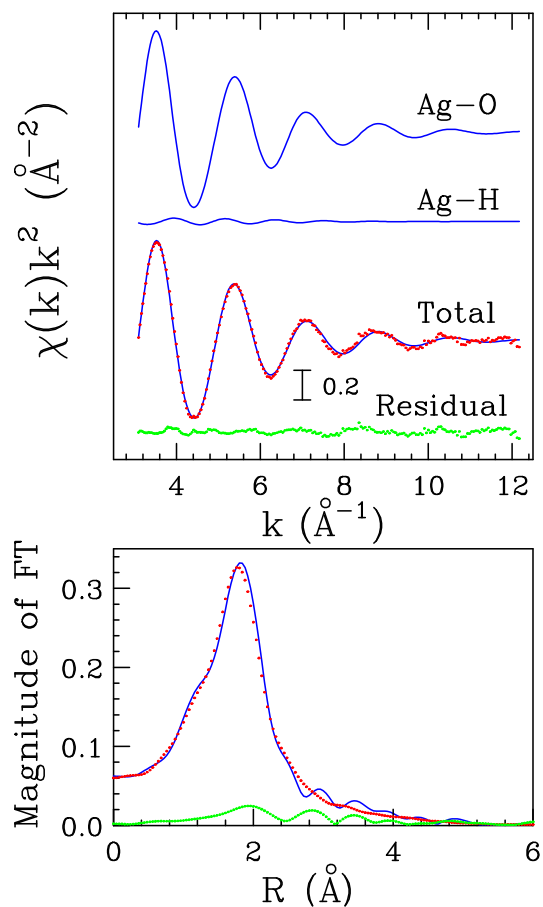


Figure 2: Upper panel: analysis of the Ag K-edge EXAFS spectrum of the  $0.2 \text{ mol} \cdot \text{dm}^{-3}$   $\text{AgClO}_4$  aqueous solution with  $\text{CN}=2$ . From the top the best fit theoretical Ag-O and Ag-H two-body contributions are shown, as well as the total theoretical signal (blue line) together with the experimental spectrum (red dots) and the corresponding residuals (green line). Lower panel: non-phase shift corrected Fourier Transforms of the best-fit EXAFS theoretical signal (blue line) of the experimental data (red dots) and of the residual curve (green line).

The mean Ag-O bond distance resulted to be 2.34(2) Å (Table 1) and this value is in good agreement with previous experimental determinations reported in the literature ranging between 2.31 and 2.42 Å,<sup>3,4,7</sup> while the Ag-H distance of 3.02(2) Å is reasonable taking into account the geometry of the water molecule. The tetrahedrally-distorted-to-linear "2 + 2" model<sup>7</sup> has also been tested in the EXAFS fit, however the two-body signal associated with two additional Ag-O paths arising from two distal oxygen atoms initially placed at 2.48 Å resulted in a theoretical signal with negligible amplitude. Finally, it worths mentioning that a theoretical signal coming from the linear O-Ag-O MS path was also included in the fit, but it turned out to provide a negligible contribution to the EXAFS oscillation in agreement with what found by Persson and co-workers.<sup>7</sup> Such kind of three body distributions have been observed to provide non-negligible contributions to the EXAFS oscillation in case of well-defined metal ions hydration complexes such as for example the Zn<sup>+2</sup>, Co<sup>+2</sup> and Ni<sup>+2</sup> cases.<sup>60-62</sup> In such species, detectable MS signals have been found for three body configurations involving collinear distributions due to the so-called "focusing effect" and to the presence of three O-metal-O linear contributions within the octahedral complex.<sup>34,39</sup> Here, the O-Ag-O three body distribution has been found to provide a negligible amplitude due to the quite long Ag-O distance of 2.34(2) Å (Table 1) and to the presence of a single MS linear contribution as compared to other transition metal ions.<sup>60-62</sup>

## **Determination of Ag<sup>+</sup> hydration structure by XANES**

Several cluster models have been used in the past to describe the coordination of Ag<sup>+</sup> in water and among them 4- and 6-fold complexes are the most accepted ones based on both experimental and theoretical results.<sup>3-6,8,12-17,64</sup> However, a unified picture on the structure of the Ag<sup>+</sup> hydration complex has not been reached yet due the difficulty of the experimental and theoretical approaches used so far in determining the structure of cations having non-symmetrical coordinations. Our EXAFS analysis suggests that the Ag<sup>+</sup> ion in water tends to coordinate with two water molecules that are likely to form a linear complex similarly to the configurations observed at the solid state.<sup>20-23,25</sup> Here, the XANES technique has been used to verify this hypothesis as this is the most suited tech-



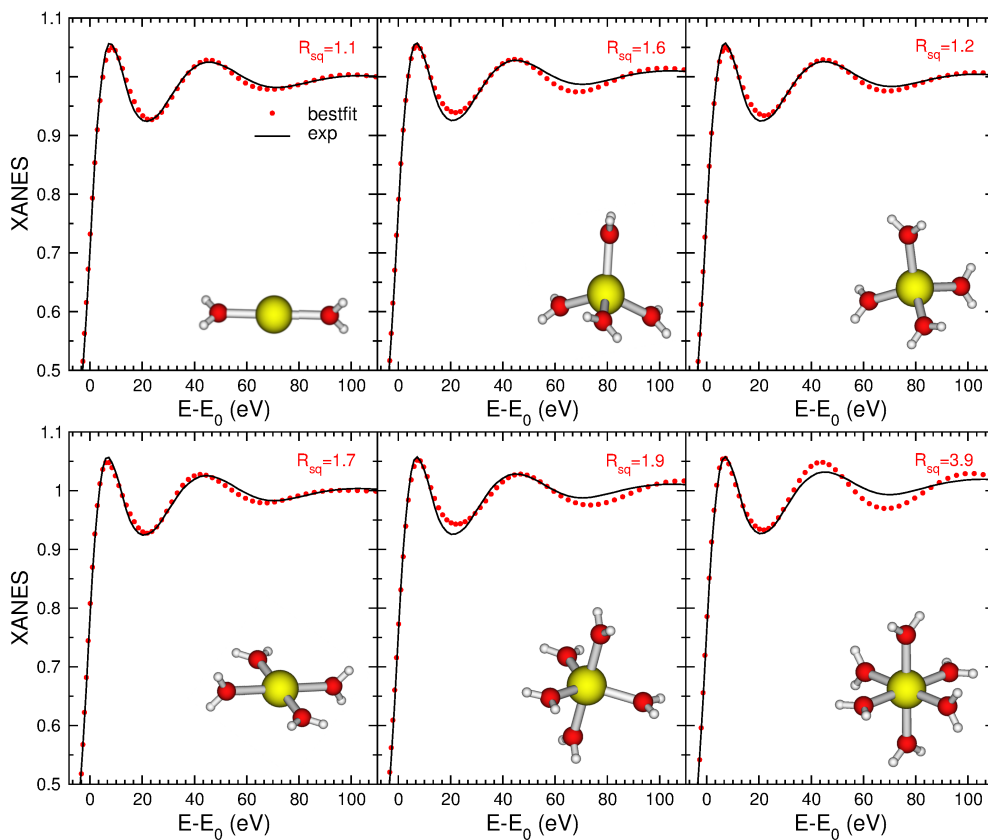


Figure 3: Comparison of the XANES K-edge experimental spectrum collected on a  $0.2 \text{ mol} \cdot \text{dm}^{-3}$   $\text{AgClO}_4$  aqueous solution (black line) with the theoretical ones (red dots) optimized by starting from clusters with different  $\text{Ag}^+$  coordination numbers. From top-left to bottom-right: CN = 2 (linear), CN = 4 (tetrahedral), "2+2" model (linearly-distorted tetrahedral), CN = 4 (square-planar), CN = 5 (trigonal bipyramid) and 6 (octahedral). For each fitting procedure, the obtained residual function  $R_{sq}$  and the cluster corresponding to the optimized structural parameters are shown as insets.

nique to determine the structure of metal complexes in solution. At variance with EXAFS the atomic thermal and structural disorder has an almost negligible effect on the low  $k$  region of the XAS spectra while MS paths provide a much bigger contribution.<sup>65</sup> Thus XANES can provide complementary information and in principle, a complete recovery of the three-dimensional arrangement of the scattering atoms around the photoabsorber can be obtained by means of XANES analysis. Therefore, to further confirm the results obtained so far a fitting procedure has been applied to the XANES spectrum of the  $0.2 \text{ mol} \cdot \text{dm}^{-3}$   $\text{AgClO}_4$  aqueous solution starting from clusters with different coordination numbers and symmetry. Besides the linear coordination (CN = 2), clusters with four water molecules have been employed as starting models by taking into account both the "2+2" tetrahedrally-distorted-to-linear geometry<sup>7</sup> and clusters with four waters arranged in a tetrahedral fashion around the  $\text{Ag}^+$  ion, as well as in a square-planar geometry. In addition, to further test the possible occurrence in solution of CNs higher than four, clusters with CNs of 5 (trigonal bipyramidal) and 6 (octahedral) geometries have been employed. The results of the fitting procedures are shown in Figure 3 while the best-fit structural and nonstructural parameters are listed in Table 2.

**Table 2: Structural and non-structural parameters obtained from the XANES analysis for the tested complexes. CN is the coordination number, R is the Ag-O distance,  $E_0$  the threshold energy,  $E_F$  the Fermi energy level,  $\Gamma_{exp}$  the experimental resolution,  $E_s$  and  $A_s$  are the energy and amplitude of the plasmon, respectively.**

	CN	R (Å)	$E_0$ (eV)	$E_F$ (eV)	$\Gamma_{exp}$ (eV)	$E_s$ (eV)	$A_s$
Linear	2	2.36(3)	8.4	-3.2	4.3	7.0	7.1
Tetrahedral	4	2.37(3)	8.5	-3.9	4.3	8.3	11.0
"2+2" model	4	2.32(3)-2.54(3)	8.3	-4.1	3.9	7.1	10.1
Square-planar	4	2.36(3)	8.5	-8.2	4.2	8.5	12.2
Trigonal bipyramid	5	2.35(3)	8.2	-6.8	4.1	9.1	11.2
Octahedral	6	2.35(3)	8.5	-6.7	4.1	9.8	11.4

As can be observed, the best fit was provided by the cluster with CN = 2, and for this model two water molecules have been optimized assuming a linear geometry around the  $\text{Ag}^+$  ion. This coordination shows a very good agreement between the experimental and theoretical spectra, as pointed out by the residual function value  $R_{sq} = 1.1$  and the Ag-O distance obtained from the

minimization procedure (2.36(3) Å) is in very good agreement with the EXAFS determination. Differently,  $R_{sq}$  increases for higher CNs up to a very poor fit obtained for coordination numbers of 5 and 6. In particular, here a clear mismatch in the first and third oscillations after the threshold energy can be observed. Altogether these results show that XANES confirms the preference for the linear coordination of the  $\text{Ag}^+$  ion in aqueous solution already suggested by the analysis of the EXAFS part of the spectrum. Instead, a special mention has to be devoted to the "2+2" model. In fact, it has to be noted that this model provided a  $R_{sq}$  of 1.2 and therefore a fit that is not much worse than that obtained with the linear configuration (Figure 3). This result suggests that the presence of additional water molecules set at distances that are longer than those of the first hydration shell as found by the EXAFS analysis (Table 1), but still closer than a hypothetical second hydration sphere, cannot be excluded. However, the combined results of the EXAFS and XANES analysis show that it is not possible to establish a definite geometry of these additional water molecules around  $\text{Ag}^+$ . This suggests that a high amount of configurational disorder is present beyond the metal ion first hydration shell, this disorder being responsible for the negligible contribution to the XAS amplitude provided by water molecules that are set at distances longer than the first coordinating ones. In fact, the high mobility of such additional waters in solution is traduced in high Debye-Waller factors and in a flattening of the XAS signal related to these photoelectron paths. This is qualitatively in agreement with what was found by Persson and co-workers by means of EXAFS and LAXS, where the authors suggested that a certain amount of water molecules could be present at distances slightly longer than the first hydration shell, even if they pointed out that it was not possible to define their precise number neither a definite geometry.<sup>7</sup> Nevertheless, the results of the XANES analysis strongly suggests a low reliability for models with CNs higher than four, like the 5- and 6-fold cases, even though the formation of these clusters have been previously suggested by other authors both on the basis of EXAFS data analysis<sup>8</sup> and as a result of theoretical methods.<sup>12-16,64</sup>

## Car-Parrinello Molecular Dynamics Simulation

The structural properties of the  $\text{Ag}^+$  ion in aqueous solution have been investigated also by means of CPMD simulations. To this purpose, calculations have been carried out on a neutral system consisting of one  $\text{Ag}^+$  ion immersed in 99 water molecules and in presence of a  $\text{Cl}^-$  anion fixed in a box corner. The obtained Ag-O radial distribution function  $g(r)$  is shown in Figure 4 and compared with the Ag-O distribution obtained from the best-fit of the EXAFS data. The first feature of the CPMD  $g(r)$  that captures the attention is that the Ag-O distribution does not go to zero after the first peak, as it is usually observed for long-lived complexes of metal ions with well-defined geometries in aqueous solution.<sup>53,60–62</sup> Differently, the  $g(r)$  shown in Figure 4 suggests a non-negligible probability of finding a certain amount of water molecules between the innermost hydration shell, indicated by the first peak, and the second hydration shell, this latter corresponding to the bump between  $\sim 3.5$  and  $4.5$  Å. To obtain a more detailed description of the  $\text{Ag}^+$  first shell coordination reproduced by CPMD, the first peak of the Ag-O  $g(r)$  has been modeled with a  $\Gamma$ -like function up to a cutoff distance of  $2.5$  Å between the silver ion and water oxygen atoms. This value has been chosen in order to exclude as much as possible the contribution provided by water molecules set beyond the first hydration shell. The obtained parameters are reported in Table 3, while the fitting  $\Gamma$ -function is shown in Figure S2. From the values in Table 3 it can be observed that the CPMD simulation provides a very asymmetric Ag-O distribution, as highlighted by the value of  $\beta$  which is 0.8. As a consequence, the maximum  $R_{max}$ , which is located at  $2.29$  Å, is relatively far from the average value  $R$  obtained at  $2.37$  Å after the fitting procedure. This value is in very good agreement with the average Ag-O bond distance obtained from the EXAFS fitting (Table 1), also by taking into account XAS uncertainty on distances of  $\pm 0.02$  Å. The total coordination number for the first peak reports an average value of 2.3 water molecules around the  $\text{Ag}^+$  ion and a Debye-Waller factor of  $0.019$  Å<sup>2</sup> is also obtained. Altogether these results show how the CPMD simulation was able to reproduce a  $\text{Ag}^+$  coordination in aqueous solution in very good agreement with the EXAFS data analysis for what concerns the first hydration shell (Table 1), as can also be observed by the good match between the two Ag-O distributions compared in

Figure 4.

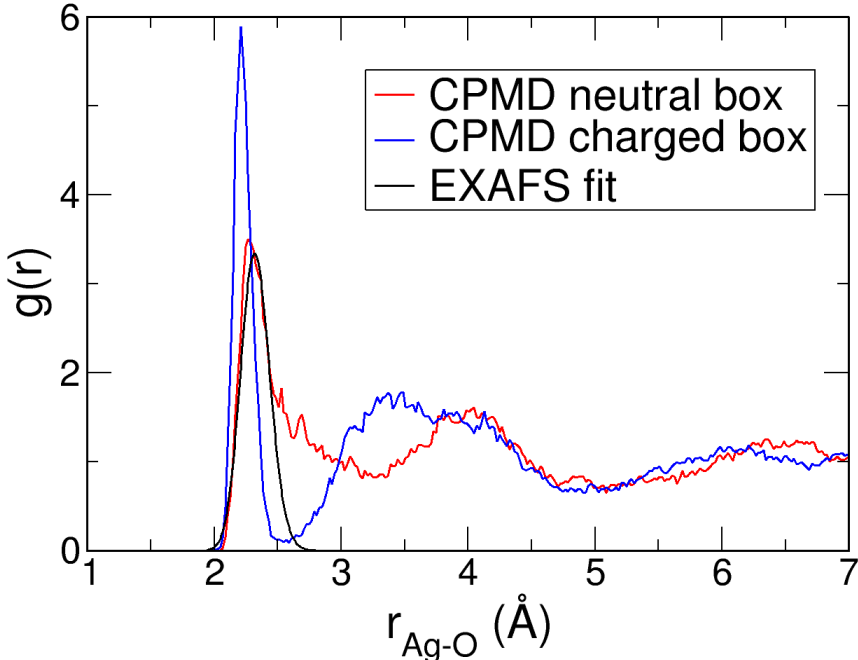


Figure 4: Ag-O radial distribution function  $g(r)$  calculated from the CPMD simulation (red line) compared with the Ag-O distribution obtained from the best-fit of the EXAFS Ag K-edge spectrum of the  $0.2 \text{ mol}\cdot\text{dm}^{-3}$   $\text{AgClO}_4$  aqueous solution (black line).

**Table 3: Coordination number CN, first maximum position  $R_{max}$ , first peak average value R, Debye-Waller factor  $\sigma^2$  and peak asymmetry  $\beta$  of the CPMD Ag-O  $g(r)$  as obtained by modeling the first peak with a  $\Gamma$ -like function.**

CN	$R_{max}$ (Å)	R (Å)	$\sigma^2$ (Å <sup>2</sup> )	$\beta$
2.3	2.29	2.37	0.019	0.8

An important issue that we would like to address is related to the employment of the system with the total positive charge, consisting in a simulation box of one  $\text{Ag}^+$  ion and 100 water molecules. The Ag-O  $g(r)$  obtained from this simulation is shown in Figure 4 and compared with that from the CPMD calculation with the neutral box and from the Ag-O distribution obtained with the EXAFS data fit. At first glance, it can be noted a clear mismatch between this  $g(r)$  and the experimental one. In addition, the Ag-O distribution goes to zero after the first peak, differently from the  $g(r)$  calculated from the simulation of the neutral box. This highlights that in the positively-charged system there are no water molecules at a distance from silver comprised be-

tween the first and second hydration shells. Also in this case, the first peak has been modeled with a  $\Gamma$ -like function. The obtained fit is shown in Figure S3, while the fitting parameters are reported in Table S2. As can be observed, the first peak integrates a total of 2.0 water molecules, and a quite asymmetrical distribution ( $\beta = 0.6$ ) is also obtained, provoking a shift of the average bond distance from the maximum  $R_{max} = 2.20 \text{ \AA}$  to the average value  $R = 2.24 \text{ \AA}$ . However, the peculiar characteristic of this distribution is that a dramatically small Debye-Waller factor of  $0.006 \text{ \AA}^2$  is obtained, thus much smaller with respect to the CPMD simulation performed on the neutral system ( $\sigma^2 = 0.019 \text{ \AA}^2$ , Table 3) and from the EXAFS fit ( $\sigma^2 = 0.013 \text{ \AA}^2$ , Table 1). This highlights how the interaction between the  $\text{Ag}^+$  ion and water is much more rigid in the case of the CPMD simulation with the charged box, as can clearly be observed also from the comparison between the different  $g(r)$ s in Figure 4, showing a much more intense distribution with respect to the experimental one and to the simulation of the neutral box. This effect has to be attributed to the lack of charge neutralization, probably resulting in a contraction due to the positive charge and, consequently, to an over-structuration of the silver-water interaction. Interestingly, from the comparison in Figure S2 it can be observed that also the bump connected with the second hydration shell around silver is found at shorter distances with respect to the CPMD simulation of the neutral system, thus suggesting a contraction of the whole bulk water structure in the charged system. It has to be noted that in both systems the box side length has been chosen in order to reproduce pure water density at 300 K. MD simulations of metal cations in water are often performed without the introduction of counter-anions or charge correction. This approximation might be negligible for classical MD simulations where boxes of several tens of Angstroms are built, but its effect can be important for *ab initio* MD where the high computational effort of the method often forces to perform simulations on systems that are not much bigger than a 10 - 20  $\text{\AA}$  side box.

To get more insights into the three-dimensional arrangement of water molecules around the  $\text{Ag}^+$  ion provided by CPMD, a combined distribution function (CDF) between distances and angles distributions has been calculated from the simulation of the neutral system. It is well-known that the identification of the local three-dimensional structures that are formed around ions in liquid

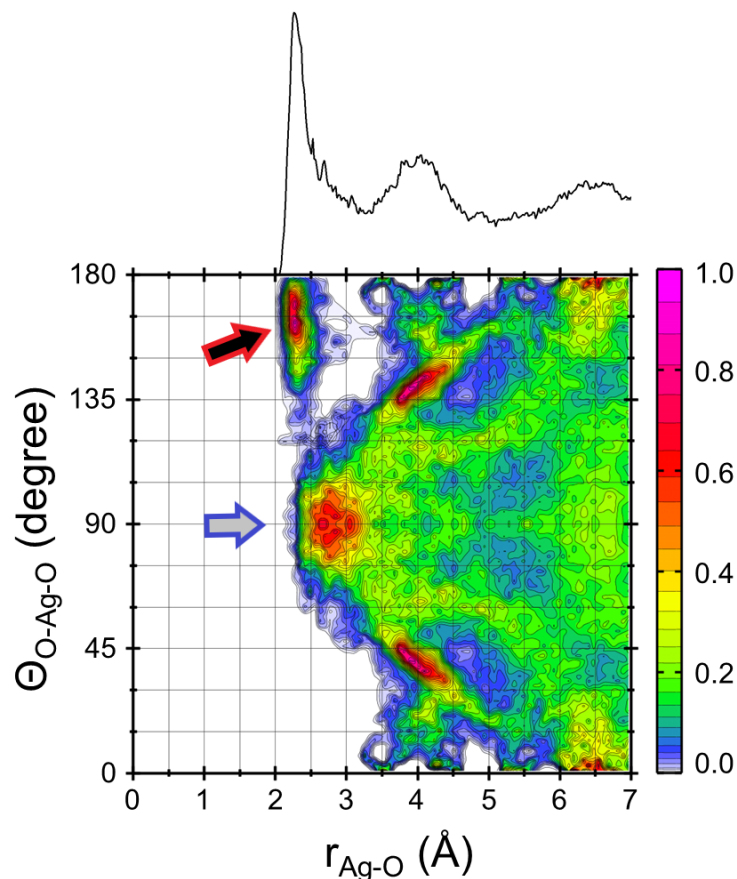


Figure 5: Combined distribution function (CDF) between Ag-O distances and O-Ag-O angles calculated from the CPMD simulation. The first area on top-left (red arrow) is referred to the intramolecular distribution between silver(I) and the two first shell coordinating waters, with angles formed between the two vectors pointing from  $\text{Ag}^+$  to each of the two first shell waters oxygens. The remaining of the surface (blue arrow) is referred to the rest of water molecules with the exclusion of the first shell ones, with angles calculated between the vector going from  $\text{Ag}^+$  to one of the first shell coordinating oxygens, that was taken as reference, and vectors connecting  $\text{Ag}^+$  with outer-shells oxygen atoms. The color-box on the right side is relative to the probability function of finding the inspected particle at that distance and angle normalized to one. The correspondent Ag-O radial distribution function  $g(r)$  is also shown on top for sake of clarity.

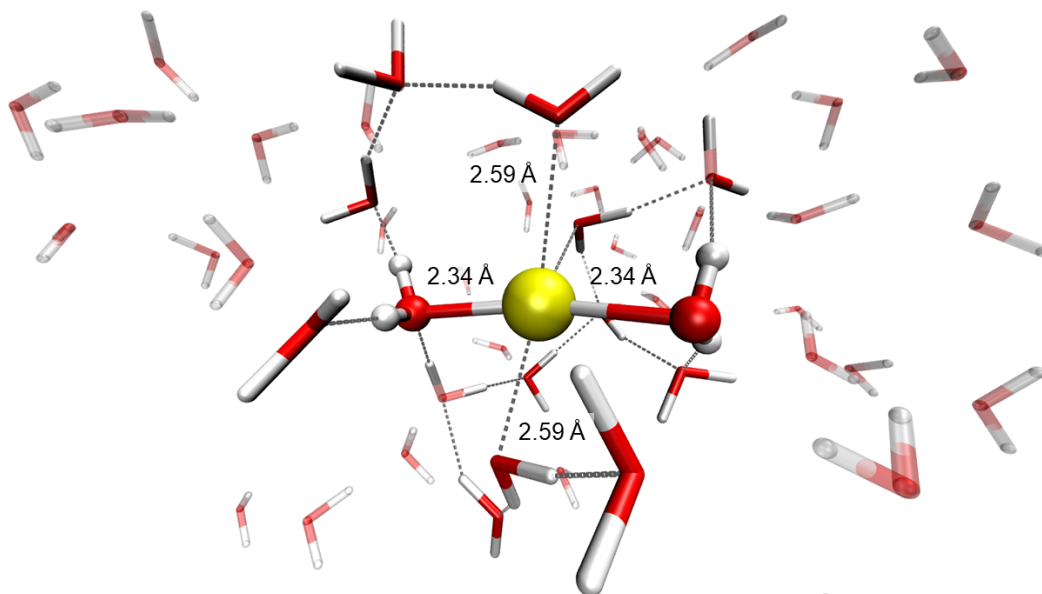


Figure 6: Representative snapshot taken from the CPMD simulation:  $\text{Ag}^+$  ion and the first coordination shell (balls and sticks), second-shell (opaque licorice), and bulk (transparent). The hydrogen-bonds network between water molecules up to the second hydration shell as well as the interaction of waters set beyond the first coordinating ones with silver are highlighted by the gray dotted lines.

systems can be a very difficult task, in particular owing to the thermal and structural disorder often displayed in these media.<sup>34,35</sup> In this framework, CDFs can be much more informative than commonly employed radial or angular distribution functions alone, as they provide information on distance-angle correlations that can be essential to isolate the spatial contributions of the different parts of a radial distribution function.<sup>66</sup> To this purpose, a CDF combining the Ag-O  $g(r)$  and the O-Ag-O angular distribution has been calculated. In particular, an intramolecular CDF was calculated for the two water molecules that were found to coordinate  $\text{Ag}^+$  in the first hydration shell, with angles formed between the two vectors pointing from  $\text{Ag}^+$  to each of the two first shell waters oxygen atoms. In addition, a CDF giving information about outer-sphere waters has also been calculated with angles formed between the vector going from  $\text{Ag}^+$  to one of the first shell coordinating oxygens, that was kept fixed, and vectors of instantaneous definition connecting  $\text{Ag}^+$  with outer-shells oxygen atoms. These angles were plotted against the Ag-O distances between the  $\text{Ag}^+$  ion and oxygen atoms of water beyond the first hydration shell. The obtained CDF is shown in



Figure 5, where the correspondent Ag-O  $g(r)$  is also plotted on top for the sake of clarity. As can be observed, a first area of high probability is present for distances comparable with the first  $g(r)$  peak and angles between  $150^\circ$  and  $180^\circ$  (red arrow). This contribution can be easily associated to the two first shell water molecules that, according to this CDF, are able to coordinate  $\text{Ag}^+$  assuming a linear or quasi-linear geometry. In fact, angles of values even lower than  $180^\circ$  are possible, suggesting an oscillation of the bond angle around the equilibrium value across simulation time. This result is in line with the EXAFS analysis, where a negligible contribution from the three body MS signal related to the O-Ag-O distribution has been found.

Moving forward from the first hydration shell, a second area of high probability can be observed for distances between  $\sim 2.5$  and  $3.25 \text{ \AA}$  and O-Ag-O angles around  $90^\circ$  (blue arrow). As can be observed from the comparison with the  $g(r)$  shown on top, this area is found at distances comprised between the Ag-O first peak and the broad bump of the second hydration shell. In particular, water molecules connected with this area are those providing an Ag-O  $g(r)$  that does not go to zero after the first peak, as it was previously reported (Figure 4). A certain amount of water molecules is therefore able to approach the  $\text{Ag}^+$  ion at distances that are longer than the average bond length formed with the two first-shell water molecules, but shorter than the second hydration sphere. In addition, from the CDF in Figure 5 it can also be observed that these water molecules assume a perpendicular arrangement with angles close to  $90^\circ$  with respect to the linear O-Ag-O axis formed by first shell water molecules. This result suggests a picture in which the  $\text{Ag}^+$  ion is mainly coordinated by the two first-shell water molecules assuming a quasi-linear coordination, with the presence of additional water molecules that can occupy a region of space set between this first hydration sphere and the second shell. It is reasonable to suppose that these waters can both weakly-interact with the  $\text{Ag}^+$  and partially be embedded in the hydrogen-bonds network with waters of the second hydration shell. This picture is confirmed also by the analysis of the instantaneous Ag-O coordination number calculated for a shell up to  $2.5 \text{ \AA}$  (Figure S4), where the number of water molecules found among this cutoff distance is predominant for 2-fold coordination (77.8%), but smaller percentages are also obtained for other CN values up to a number

of four water molecules. Reasonably, these waters are responsible for the contribution to the CN value of 2.3, thus higher than two, obtained after the fitting procedure of the Ag-O  $g(r)$  (Table 3). The impossibility in determining if a proper coordination with silver occurs, or if the water-water interaction has a dominant role in such case, is in line with the weak hydration extent of  $\text{Ag}^+$  in aqueous solution. In addition, the fact that for the two first shell molecules also bond angles below  $180^\circ$  have been obtained may arise from the occasional interaction of these additional waters with the  $[\text{Ag}(\text{H}_2\text{O})_2]^+$  species, causing a bend in the O-Ag-O angle during the approach. Note that this area of the CDF can be reasonably associated to water with such a behavior instead of being connected with exchange processes between the first and second hydration shells, as only two events of this kind have been observed to occur during the 35 ps trajectory. However, the short simulation times that are typical of *ab initio* MD prevent a thorough study of water residence time in the  $\text{Ag}^+$  coordination sphere, even though some authors have already pointed out that rapid exchange processes between the first and second hydration shells of this metal ion may occur.<sup>12,16</sup> In Figure 5 two areas of high probability are found for distances between  $\sim 3.5$  and  $4.5 \text{ \AA}$  and angles of respectively of  $45^\circ$  and  $135^\circ$ . Still by the comparison with the  $g(r)$  shown on top, it comes clear that these waters belong to the second hydration sphere indicated by the broad bump found within these Ag-O distances. In addition, the formed O-Ag-O angles suggest that these are water molecules interacting by means of hydrogen-bonds with the first shell coordinating waters. This is in line with the LAXS determination of Persson and co-workers, who found a second hydration sphere at  $4.76(2) \text{ \AA}$  and characterized by a broad distribution that these authors ascribed to the broad distance distribution of the inner-sphere waters<sup>7</sup> which, as a matter of fact, should imply also those waters comprised between the first and second hydration spheres that causes the high degree of disorder. An immediate view of the whole picture obtained by CPMD can be achieved by looking at the representative snapshot in Figure 6.

The obtained picture is in agreement with that provided by the XAS results and in particular by the analysis of the XANES data, where it was shown that the best-fit was obtained for two linearly-coordinated water molecules (Figure 3), but where it was also found that the presence of

additional water molecules at distances slightly longer than the bond one can not be excluded, even if it is difficult to stress a defined geometry because of a very disordered situation. Therefore, the CPMD simulation is able to further confirm this fluxional picture, also giving more insights for what concerns the presence of these water molecules set beyond the first hydration shell, that are clearly responsible for the configurational disorder around the  $\text{Ag}^+$  ion.

## Large Angle X-ray Scattering

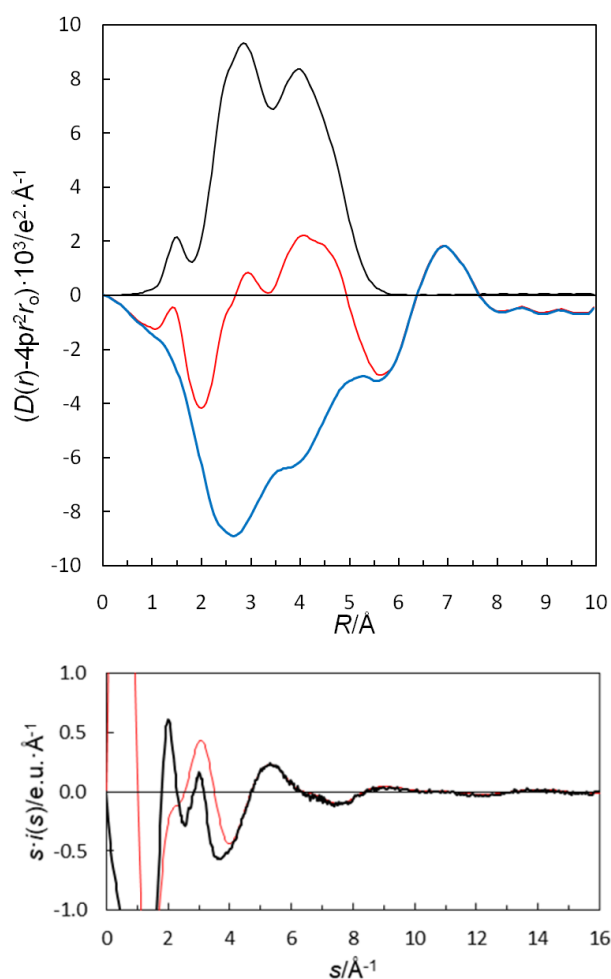


Figure 7: (Top) LAXS radial distribution curves for a  $2.0 \text{ mol} \cdot \text{dm}^{-3}$  silver(I) perchlorate aqueous solution acidified with  $0.1 \text{ mol} \cdot \text{dm}^{-3}$  perchloric acid. Upper part: Experimental radial distribution curves:  $D(r) - 4\pi r^2 \rho_0$  (red line), sum of model contributions (black line) and difference (blue line). (Bottom) Reduced LAXS intensity functions  $s \cdot i_{exp}(s)$  (black line); model  $s \cdot i_{calc}(s)$  (red line)

The LAXS data of an acidified  $2.0 \text{ mol} \cdot \text{dm}^{-3}$  aqueous silver perchlorate solution presented and

**Table 4: Mean bond distances,  $R$  ( $\text{\AA}$ ), number of distances,  $N$ , temperature coefficients,  $b$  ( $\text{\AA}^2$ ), and the half-height full width,  $l$  ( $\text{\AA}$ ), in the LAXS studies of the hydrated  $\text{Ag}^+$  ion in aqueous solution at ambient room temperature;  $O_{II}$  denotes second hydration sphere.**

Species	Interaction	N	R	b	l
$\text{Ag}(\text{H}_2\text{O})_2(\text{H}_2\text{O})_8^+$	Ag-O	2	2.32(1)	0.011(2)	0.15(1)
	Ag-O	2	2.59(2)	0.015(2)	0.17(2)
	Ag-O	6	4.04(2)	0.051(4)	0.32(1)
	Ag... $O_{II}$	4	4.65(2)	0.042(3)	0.29(1)
	(Ag-) $O$ ... $O_{II}$	2	2.81(2)	0.025(4)	0.22(2)
$\text{ClO}_4(\text{H}_2\text{O})_{12}^-$	Cl-O	4	1.453(2)	0.0031(2)	0.078(2)
	(Cl-) $O$ ... $O_{aq}$	3	3.04(4)	0.024(2)	0.22(1)
	(Cl-) $O$ ... $O_{aq}$	12	3.70(4)	0.050(2)	0.32(1)
Bulk water	$O_{aq}$ ... $O_{aq}$	2	2.890(12)	0.020(4)	0.20(2)

analyzed in Ref.<sup>7</sup> showed a broad peak in the difference function around 4  $\text{\AA}$ . At that time it was believed that such a distance was too long to be an interaction between silver ion and water, and instead it was stated "the origin of this distance is yet uncertain, but it seems that it is oxygen-oxygen distances in water arranged in a non-classical way" and the interaction was left unrefined. In the light of the CPMD simulations in this study it is possible that such long and very weak interactions between the  $\text{Ag}^+$  ion and water exists, and may play an important and unusual role in the hydration of this ion. The LAXS data set has therefore been re-evaluated by including a Ag...OH<sub>2</sub> distance close to 4  $\text{\AA}$ . In order to make up for the broad peak in the difference function ca. six water molecules are needed. By the introduction of this distance a significantly better fit was obtained, most of the other structure parameters are slightly effected, but the main picture remains. The structure parameters of the new refinement of the LAXS data are summarized in Table 4, and the radial distribution functions and the refined intensity function are shown Figure 7. The results of the LAXS data are in full agreement with the structure parameters obtained by EXAFS and XANES (Tables 1 and 2) as well as the CPMD simulations (Figure 5).

## Conclusions

The coordination of the  $\text{Ag}^+$  ion in aqueous solution has been studied by means of XAS spectroscopy, CPMD simulations and LAXS. The analysis of the EXAFS part of the spectrum was performed for different coordination numbers of the  $\text{Ag}^+$  ion in the 1.0 - 6.0 range, and the resulting residuals between the theoretically generated and experimental spectra showed that the best-fit is obtained for a CN of 2.0 and an average Ag-O distance of 2.34(2) Å. The LAXS data give the same results, 2.32(1) Å. The analysis of the XANES part of the experimental spectrum was also performed for the first time on this case study. XANES data-fitting was carried out starting from clusters with different CNs in the 2 - 6 range and all the structural parameters were optimized during data minimization. The results showed a preference for a coordination involving two first shell water molecules in a linear arrangement. However, the acceptable results obtained with a "2 + 2" model suggest that the presence of additional water molecules set at distances only slightly longer than the bond one cannot be excluded.

CPMD simulations provided an Ag-O first shell distribution that is in very good agreement with the XAS data in terms of number of coordinating molecules, bond distances and mean square displacement. The CDF analysis provided more insights into the composition and geometry of water around  $\text{Ag}^+$  and highlighted in particular the presence of waters at distances comprised between the first and second hydration shells assuming a perpendicular configuration with respect to the O-Ag-O linear axis. These waters form a broad distribution that make them impossible to detect by the XAS signal, since the high configurational disorder is traduced in a high Debye-Waller factor and in a flattening of the XAS amplitude. This model is fully supported by the LAXS data.

The whole results provide a conclusive picture of the  $\text{Ag}^+$  hydration structure, where two water molecules are found to mainly coordinate the metal ion assuming a linear configuration. The linear diaquo-complex presents a second-shell structure of mobile water molecules which can either weakly-interact with the cation or coordinate the first shell waters through hydrogen bonds. This picture could also explain the higher number of CNs, always higher than two, that has been

observed so far for what concerns  $\text{Ag}^+$  coordination in aqueous solution. In addition, the fluxional situation found in this work show how, for certain case studies, the description of a metal ion coordination in terms of simple limit geometries is no longer reliable. The water molecules outside the linear  $[\text{Ag}(\text{H}_2\text{O})_2]^+$  core have a strong effect on the overall hydration of the  $\text{Ag}^+$  ion seen in a ca.  $0.2 \text{ \AA}$  longer Ag-O bond distance than in isolated  $[\text{Ag}(\text{H}_2\text{O})_2]^+$  ions in solid state. The hydrated  $\text{Ag}^+$  ion can be seen as a linear  $[\text{Ag}(\text{H}_2\text{O})_2]^+$  unit surrounded by a few water molecules at relatively short Ag...O distance, ca.  $2.6 \text{ \AA}$ , possibly perpendicular to the linear  $[\text{Ag}(\text{H}_2\text{O})_2]^+$  ion, and another set of water molecules as a swarm at much longer distance, ca.  $4 \text{ \AA}$

## Supporting Information

The following content is available in Supporting Information: Figure S1, Figure S2, Figure S3, Figure S4, Table S1, Table S2.

## Acknowledgments

The experimental data were collected at the Stanford Synchrotron Radiation Lightsource, SLAC National Accelerator Laboratory, which is supported by the U.S. Department of Energy, Office of Science, Office of Basic Energy Sciences under Contract No. DE-AC02-76SF00515. The SSRL Structural Molecular Biology Program is supported by the DOE Office of Biological and Environmental Research, and by the National Institutes of Health, National Institute of General Medical Sciences (P41GM103393). The contents of this publication are solely the responsibility of the authors and do not necessarily represent the official views of NIGMS or NIH. We acknowledge financial support from the Italian Ministry of University and Research (MIUR) through grant “PRIN 2017, 2017KKP5ZR, MOSCATo” and from University of Rome La Sapienza grant n. RG11916B702B43B9. This work was supported by the CINECA supercomputing centers through the Grant IscrC\_DESTINIS (n.HP10CZTDIS).

## References

- (1) Ohtaki, H.; Radnai, T. Structure and Dynamics of Hydrated Ions. *Chem. Rev.* **1993**, *93*, 1157–1204.
- (2) Marcus, Y. Effect of ions on the structure of water: Structure making and breaking. *Chem. Rev.* **2009**, *109*, 1346–1370.
- (3) Skipper, N. T.; Neilson, G. W. X-ray and neutron diffraction studies on concentrated aqueous solutions of sodium nitrate and silver nitrate. *J. Phys.: Cond. Matt.* **1989**, *1*, 4141–4154.
- (4) Sandstrom, M.; Neilson, G. W.; Johansson, G.; Yamaguchi, T. Ag<sup>+</sup> hydration in perchlorate solution. *J. Phys. C: Solid State Physics* **1985**, *18*, 1115–1121.
- (5) Yamaguchi, T.; Lindqvist, O.; Boyce, J.; Claeson, T. Determination of the hydration structure of silver ions in aqueous silver perchlorate and nitrate solutions from EXAFS using synchrotron radiation. *Acta Chem. Scand.* **1984**, *38*, 423–428.
- (6) Tsutsui, Y.; Sugimoto, K.-i.; Wasada, H.; Inada, Y.; Funahashi, S. EXAFS and ab Initio Molecular Orbital Studies on the Structure of Solvated Silver(I) Ions. *J. Phys. Chem. A* **1997**, *101*, 2900–2905.
- (7) Persson, I.; Nilsson, K. B. Coordination Chemistry of the Solvated Silver(I) Ion in the Oxygen Donor Solvents Water, Dimethyl Sulfoxide, and N,N-Dimethylpropyleneurea. *Inorg. Chem.* **2006**, *45*, 7428–7434.
- (8) Fulton, J. L.; Kathmann, S. M.; Schenter, G. K.; Balasubramanian, M. Hydrated Structure of Ag(I) Ion from Symmetry-Dependent, K- and L-Edge XAFS Multiple Scattering and Molecular Dynamics Simulations. *J. Phys. Chem. A* **2009**, *113*, 13976–13984.
- (9) Di Bernardo, P.; Melchior, A.; Portanova, R.; Tolazzi, M.; Zanonato, P. L. Complex formation of N-donor ligands with group 11 monovalent ions. *Coord. Chem. Rev.* **2008**, *252*, 1270–1285.

- (10) Fox, B. S.; Beyer, M. K.; Bondybey, V. E. Coordination Chemistry of Silver Cations. *J. Am. Chem. Soc.* **2002**, *124*, 13613–13623.
- (11) Antolovich, M.; Lindoy, L. F.; Reimers, J. R. Explanation of the Anomalous Complexation of Silver(I) with Ammonia in Terms of the Poor Affinity of the Ion for Water. *J. Phys. Chem. A* **2004**, *108*, 8434–8438.
- (12) Armunanto, R.; Schwenk, C. F.; Rode, B. M. Structure and Dynamics of Hydrated Ag (I): Ab Initio Quantum Mechanical-Molecular Mechanical Molecular Dynamics Simulation. *J. Phys. Chem. A* **2003**, *107*, 3132–3138.
- (13) Dubois, V.; Archirel, P.; Boutin, A. A Monte Carlo Simulations of Ag<sup>+</sup> and Ag in Aqueous Solution. Redox Potential of the Ag<sup>+</sup>/Ag Couple. *J. Phys. Chem. B* **2001**, *105*, 9363–9369.
- (14) Spezia, R.; Nicolas, C.; Archirel, P.; Boutin, A. Molecular dynamics simulations of the Ag<sup>+</sup> or Na<sup>+</sup> cation with an excess electron in bulk water. *J. Chem. Phys.* **2004**, *120*, 5261–5268.
- (15) Vuilleumier, R.; Sprik, M. Electronic properties of hard and soft ions in solution: Aqueous Na<sup>+</sup> and Ag<sup>+</sup> compared. *J. Chem. Phys.* **2001**, *115*, 3454–3468.
- (16) Blauth, C. M.; Pribil, A. B.; Randolf, B. R.; Rode, B. M.; Hofer, T. S. Structure and dynamics of hydrated Ag<sup>+</sup>: An ab initio quantum mechanical/charge field simulation. *Chem. Phys. Lett.* **2010**, *500*, 251 – 255.
- (17) Leung, K.; Rempe, S. B.; Von Lilienfeld, O. A. Ab initio molecular dynamics calculations of ion hydration free energies. *J. Chem. Phys.* **2009**, *130*.
- (18) Li, P.; Song, L. F.; Merz, K. M. Systematic parameterization of monovalent ions employing the nonbonded model. *J. Chem. Theo. Comput.* **2015**, *11*, 1645–1657.
- (19) Kumar, M.; Francisco, J. S. Evidence of the Elusive Gold-Induced Non-classical Hydrogen Bonding in Aqueous Environments. *J. Am. Chem. Soc.* **2020**, *142*, 6001–6006.



- (20) Makhmudova, N.K. and Sharipov, Kh.T. and Khodashova, T.S. and Porai-Koshits, M.A. and Parpiev, N.A., -. *Doklady Akademii Nauk SSSR* **1985**, 280, 1360.
- (21) Zhao, L.; Mak, T. C. W. Assembly of Silver(I) Two- and Three-Dimensional Coordination Networks with Complementary Tridentate Heteroaryl Ethynide Ligands. *Inorg. Chem.* **2009**, 48, 6480–6489.
- (22) Wu, H.; Dong, X.-W.; Ma, J.-F.; Liu, H.-Y.; Yang, J.; Bai, H.-Y. Influence of anionic sulfonate-containing and nitrogen-containing mixed-ligands on the structures of silver coordination polymers. *Dalton Trans.* **2009**, 0, 3162–3174.
- (23) Li, Y.-J.; Dong, X.-W.; Wu, H. Diaquasilver(I) 6-aminonaphthalene-1-sulfonate monohydrate. *Acta Cryst. Sec. E* **2007**, 63, 2230.
- (24) Liu, H.-Y.; Wu, H.; Ma, J.-F.; Song, S.-Y.; Yang, J.; Liu, Y.-Y.; Su, Z.-M. Structural Study of Silver(I) Sulfonate Complexes with Pyrazine Derivatives. *Inorg. Chem.* **2007**, 46, 7299–7311, PMID: 17685508.
- (25) Wang, G.-H.; Li, Z.-G.; Jia, H.-Q.; Hu, N.-H.; Xu, J.-W. Constructing mixed-metal coordination polymers from copper(II)–pyridinedicarboxylate metalloligands. *Acta Cryst. Sec. C* **2009**, 65, m333–m336.
- (26) Mazej, Z.; Goreshnik, E. Crystal structures of  $[\text{SbF}_6]^-$  salts of di- and tetrahydrated  $\text{Ag}^+$ , tetrahydrated  $\text{Pd}^{2+}$  and hexahydrated  $\text{Cd}^{2+}$  cations. *Zeits. Kristall. - Crystal. Mater.* **2017**, 232, 339 – 347.
- (27) Li, B.; Zang, S.-Q.; Li, H.-Y.; Wu, Y.-J.; Mak, T. C. Diverse intermolecular interactions in silver(I)-organic frameworks constructed with flexible supramolecular synthons. *J. Organom. Chem.* **2012**, 708-709, 112 – 117.
- (28) Malischewski, M.; Peryshkov, D. V.; Bukovsky, E. V.; Seppelt, K.; Strauss, S. H. Structures of  $\text{M}_2(\text{SO}_2)_6\text{B}_{12}\text{F}_{12}$  ( $\text{M} = \text{Ag}$  or  $\text{K}$ ) and  $\text{Ag}_2(\text{H}_2\text{O})_4\text{B}_{12}\text{F}_{12}$ : Comparison of the Coordination

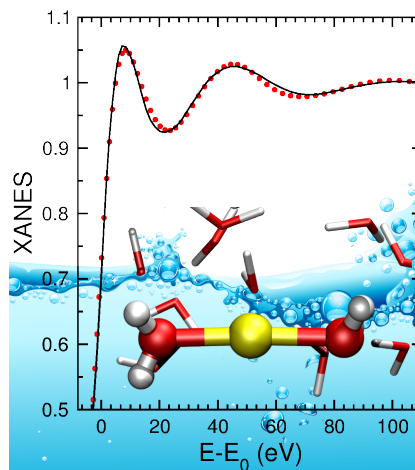
- of SO<sub>2</sub> versus H<sub>2</sub>O and of B<sub>12</sub>F<sub>12</sub> versus Other Weakly Coordinating Anions to Metal Ions in the Solid State. *Inorg. Chem.* **2016**, *55*, 12254–12262, PMID: 27934406.
- (29) Molinier, M.; Massa, W. New Fluoromanganate(III) Hydrates: Mn<sub>3</sub>F<sub>8</sub> · 12H<sub>2</sub>O and AgMnF<sub>4</sub> · 4H<sub>2</sub>O. *Zeit. anorg. und allgem. Chemie* **1994**, *620*, 833–838.
- (30) Holland, P. M. The thermochemical properties of gas-phase transition metal ion complexes. *J. Chem. Phys.* **1982**, *76*, 4195.
- (31) Iino, T.; Ohashi, K.; Inoue, K.; Judai, K.; Nishi, N.; Sekiya, H. Infrared spectroscopy of Cu<sup>+</sup>(H<sub>2</sub>O)<sub>n</sub> and Ag<sup>+</sup>(H<sub>2</sub>O)<sub>n</sub>: Coordination and solvation of noble-metal ions. *J. Chem. Phys.* **2007**, *126*, 194302.
- (32) Feller, D.; Glendening, E. D.; de Jong, W. A. Structures and binding enthalpies of M<sup>+</sup>(H<sub>2</sub>O)<sub>n</sub> clusters, M=Cu, Ag, Au. *J. Chem. Phys.* **1999**, *110*, 1475–1491.
- (33) Lee, E. C.; Lee, H. M.; Tarakeshwar, P.; Kim, K. S. Structures, energies, and spectra of aqua-silver(I) complexes. *J. Chem. Phys.* **2003**, *119*, 7725–7736.
- (34) Filipponi, A.; D'Angelo, P. *X-Ray Absorption and X-Ray Emission Spectroscopy*; John Wiley I& Sons, Ltd, 2016; Chapter 25, pp 745–771.
- (35) Di Cicco, A. EXAFS in liquids and disordered systems: a personal review. *XAS Res. Rev.* **2016**, *15*, 1–7.
- (36) Muñoz-Páez, A.; Sánchez Marcos, E. Molecular Structure of Solvates and Coordination Complexes in Solution as Determined with EXAFS and XANES. *Comprehensive Inorganic Chemistry II (Second Edition): From Elements to Applications* **2013**, *9*, 133–159.
- (37) Thompson, A. *X-ray Data Booklet*; Lawrence Berkeley National Laboratory, University of California, 2001.
- (38) Filipponi, A.; Di Cicco, A. X-ray-absorption spectroscopy and n-body distribution functions in condensed matter. I. Theory. *Phys. Rev. B* **1995**, *52*, 15122–15134.

- (39) Filipponi, A.; Di Cicco, A. X-ray-absorption spectroscopy and n-body distribution functions in condensed matter. II. Data analysis and applications. *Phys. Rev. B* **1995**, *52*, 15135–15149.
- (40) Hedin, L.; Lundqvist, S. Effects of Electron-Electron and Electron-Phonon Interactions on the One-Electron States of Solids. *Solid State Phys.* **1970**, *23*, 1–181.
- (41) Ravel, B. Muffin-tin potentials in EXAFS analysis. *J. Synch. Rad.* **2015**, *22*, 1258–1262.
- (42) Benfatto, M.; Della Longa, S. Geometrical fitting of experimental XANES spectra by a full multiple-scattering procedure. *J. Synch. Rad.* **2001**, *8*, 1087–1094.
- (43) CPMD V4.1 Copyright IBM Corp 1990-2015, Copyright MPI fuer Festkoerperforschung Stuttgart 1997-2001.
- (44) Becke, A. D. Density-functional exchange-energy approximation with correct asymptotic behavior. *Phys. Rev. A* **1988**, *38*, 3098–3100.
- (45) Lee, C.; Yang, W.; Parr, R. G. Development of the Colle-Salvetti correlation-energy formula into a functional of the electron density. *Phys. Rev. B* **1988**, *37*, 785–789.
- (46) Grimme, S. Semiempirical GGA-type density functional constructed with a long-range dispersion correction. *J. Comput. Chem.* **2006**, *27*, 1787–1799.
- (47) Troullier, N.; Martins, J. L. Efficient pseudopotentials for plane-wave calculations. *Phys. Rev. B* **1991**, *43*, 1993–2006.
- (48) Kleinman, L.; Bylander, D. M. Efficacious Form for Model Pseudopotentials. *Phys. Rev. Lett.* **1982**, *48*, 1425–1428.
- (49) Silvestrelli, P. L.; Parrinello, M. Structural, electronic, and bonding properties of liquid water from first principles. *J. Chem. Phys.* **1999**, *111*, 3572–3580.

- (50) Sprik, M.; Hutter, J.; Parrinello, M. Ab initio molecular dynamics simulation of liquid water: Comparison of three gradient-corrected density functionals. *J. Chem. Phys.* **1996**, *105*, 1142–1152.
- (51) Grossman, J. C.; Schwegler, E.; Draeger, E. W.; Gygi, F.; Galli, G. Towards an assessment of the accuracy of density functional theory for first principles simulations of water. *J. Chem. Phys.* **2004**, *120*, 300–311.
- (52) Schwegler, E.; Grossman, J. C.; Gygi, F.; Galli, G. Towards an assessment of the accuracy of density functional theory for first principles simulations of water. II. *J. Chem. Phys.* **2004**, *121*, 5400–5409.
- (53) Spezia, R.; Duvail, M.; Vitorge, P.; Cartailier, T.; Tortajada, J.; Chillemi, G.; D'Angelo, P.; Gaigeot, M. P. A coupled car-parrinello molecular dynamics and EXAFS data analysis investigation of aqueous  $\text{Co}^{2+}$ . *J. Phys. Chem. A* **2006**, *110*, 13081–13088.
- (54) D'Angelo, P.; Migliorati, V.; Sessa, F.; Mancini, G.; Persson, I. XANES reveals the flexible nature of hydrated strontium in aqueous solution. *J. Phys. Chem. B* **2016**, *120*, 4114–4124.
- (55) Sessa, F.; D'Angelo, P.; Guidoni, L.; Migliorati, V. Hidden Hydration Structure of Halide Ions: an Insight into the Importance of Lone Pairs. *J. Phys. Chem. B* **2015**, *119*, 15729–15737, PMID: 26629711.
- (56) Abraham, M. J.; Murtola, T.; Schulz, R.; Pall, S.; Smith, J. C.; Hess, B.; Lindahl, E. GROMACS: High performance molecular simulations through multi-level parallelism from laptops to supercomputers. *SoftwareX* **2015**, *1-2*, 19 – 25.
- (57) Berendsen, H. J. C.; Grigera, J. R.; Straatsma, T. P. The missing term in effective pair potentials. *J. Phys. Chem.* **1987**, *91*, 6269–6271.
- (58) Humphrey, W.; Dalke, A.; Schulten, K. VMD: Visual molecular dynamics. *J. Molec. Graph.* **1996**, *14*, 33–38.

- (59) Brehm, M.; Kirchner, B. TRAVIS - A free analyzer and visualizer for monte carlo and molecular dynamics trajectories. *J. Chem. Inform. Model.* **2011**, *51*, 2007–2023.
- (60) D'Angelo, P.; Benfatto, M.; Della Longa, S.; Pavel, N. V. Combined XANES and EXAFS analysis of  $\text{Co}^{2+}$ ,  $\text{Ni}^{2+}$ , and  $\text{Zn}^{2+}$  aqueous solutions. *Phys. Rev. B* **2002**, *66*, 064209.
- (61) D'Angelo, P.; Barone, V.; Chillemi, G.; Sanna, N.; Meyer-Klaucke, W.; Pavel, N. V. Hydrogen and higher shell contributions in  $\text{Zn}^{2+}$ ,  $\text{Ni}^{2+}$ , and  $\text{Co}^{2+}$  aqueous solutions: An X-ray absorption fine structure and molecular dynamics study. *J. Am. Chem. Soc.* **2002**, *124*, 1958–1967.
- (62) Chillemi, G.; D'Angelo, P.; Pavel, N. V.; Sanna, N.; Barone, V. Development and validation of an integrated computational approach for the study of ionic species in solution by means of effective two-body potentials. The case of  $\text{Zn}^{2+}$ ,  $\text{Ni}^{2+}$ , and  $\text{Co}^{2+}$  in aqueous solutions. *J. Am. Chem. Soc.* **2002**, *124*, 1968–1976.
- (63) Migliorati, V.; D'Angelo, P. Unraveling the  $\text{Sc}^{3+}$  Hydration Geometry: The Strange Case of the Far-Coordinated Water Molecule. *Inorg. Chem.* **2016**, *55*, 6703–6711.
- (64) Spezia, R.; Nicolas, C.; Boutin, A.; Vuilleumier, R. Molecular dynamics simulations of a silver atom in water: Evidence for a dipolar excitonic state. *Phys. Rev. Lett.* **2003**, *91*, 1–4.
- (65) Benfatto, M.; Natoli, C. R.; Bianconi, A.; Garcia, J.; Marcelli, A.; Fanfoni, M.; Davoli, I. Multiple-scattering regime and higher-order correlations in x-ray-absorption spectra of liquid solutions. *Phys. Rev. B* **1986**, *34*, 5774–5781.
- (66) Sessa, F.; D'Angelo, P.; Migliorati, V. Combined distribution functions: A powerful tool to identify cation coordination geometries in liquid systems. *Chem. Phys. Lett.* **2018**, *691*, 437–443.

## For Table of Contents Only



Extended X-ray absorption fine structure (EXAFS), X-ray absorption near-edge structure (XANES), large-angle X-ray scattering (LAXS) and Car-Parrinello molecular dynamics (CPMD) provided a reliable determination of the elusive hydration structure of the Ag<sup>+</sup> ion. A linear first shell with a mean Ag-O distance of 2.34(2) Å is observed, surrounded by a few water molecules at relatively short distance, ca. 2.6 Å, and another set of waters as a swarm at ca. 4 Å.